Revision

Surface modified carbon nanomats provide cationic and anionic rectifier membranes in aqueous electrolyte media

Luthando Tshwenya [a], Budi Riza Putra [b,c], Benjamin O. Orimolade [a], Frank Marken [b], and Omotayo A. Arotiba [a,d]*

[a] *Department of Chemical Sciences, University of Johannesburg, Doornfontein, 2028, South Africa*[1]

[b] *Department of Chemistry, University of Bath, Bath BA2 7AY, UK*

[c] *Department of Chemistry, Faculty of Mathematics and Natural Sciences, Bogor Agricultural University, Bogor, West Java, Indonesia*

[d] *Centre for Nanomaterials Science Research, University of Johannesburg, South Africa*

Corresponding author: Omotayo A. Arotiba (oarotiba@uj.ac.za)

[1] *Formerly known as the Department of Applied Chemistry, University of Johannesburg, South Africa*

Abstract

Carbon nanofibers (CNFs) are converted into anionic current rectifiers by surface modification with amine functional groups using hydrothermal means (forming modified CNFs, with generation-3 poly (propylene imine) dendrimer, urea and boric acid). To confirm surface charge, morphological changes and carbon nanomat thickness, zeta potential analysis, transmission electron microscopy (TEM) and scanning electron microscopy (SEM), were used. When a dispersion of surface modified carbon nanofibers in DMF is drop-cast asymmetrically to form nanomats onto laser drilled microholes (5, 10, or 20 μm diameter) of poly (ethylene terephthalate) substrates and immersed into aqueous electrolyte solutions, anionic diode behaviour is observed (in contrast to pristine carbon nanofibers, which exhibit cationic diode behaviour). The effects of electrolyte type, ionic strength, and microhole diameter on ionic diode performance were investigated using cyclic voltammetry, chronoamperometry, and impedance spectroscopy. Future applications in desalination are proposed.

Keywords: Surface modified carbon nanofibers; carbon nanomat; ionic current rectification; ionic diode; desalination

1. Introduction

Ionic rectifiers (or ionic diodes) [1,2,3], are ion-permeable membrane-based devices consisting, for example, of nanopores that are asymmetric in terms of shape (one side is smaller than the other) and/or in terms of surface charge [4,5,6]. These devices are inspired by processes in biological membranes with nanopores that nature provides to regulate critical processes in the human body, including neuronal communication and sensory perception [7]. Applications have been suggested in desalination [8], "iontronics" [9], power generation [10], and in sensing [11]. In contrast to these nanoscale ionic rectifier systems, also rectification mechanisms based on electrolytic junctions [12] and based on effects at the micrometre scale are possible when ion semi-permeable materials are deposited asymmetrically onto substrates with microholes [13,14] or in microfluidic systems [15,16]. These membrane devices allow uni-directional flow or movement of ions (with applied potential bias), while blocking movement of counter ions. This phenomenon leads to non-linear ionic current–voltage curves. In simple terms, ionic rectifiers can convert an alternative current (AC) potential bias input into a direct current (DC) ion flux output overall equivalent to desalination [17].

For microhole devices, ionic diode properties are material dependent (dependent on semi-permeability, surface functionality, charge density, and charge mobility) as well as environment dependent (aqueous electrolyte type, ionic strength, pH, etc.). In recent studies several materials have been tested such as polymers of intrinsic microporosity (PIMs) [18], cellulose [19], graphene oxide [20], 2D-titanate nanosheets [21], partially hydrolysed polyacrylonitrile [22], as well as carbon nanofibers [23]. These materials proved to be acceptable ionic diode materials, with intrinsic nano-porosity and surface charge (sometimes tunable or switchable) sufficiently high to give rectification ratios of typically 10 to 50 (for +/- 1V bias).

The semi-permeable materials approach to ionic rectifiers offers a way towards engineering of desalination processes with low impedance due to thin ionomer coatings and high spherical ion flux towards microhole-coated substrates [24]. The extent of cation or anion perm-selectivity is linked to the transference numbers for cations and for anions. If the surface of the diode is ideally

cation permselective, the transference number of cations t_+ will be equal to 1, while the transference number of anions t_- will be equal to 0, and *vice versa* (as a function of applied bias, electrolyte composition, and ionic strength). In addition, the ionic diode performance as a rectifier is given by the rectification ratio of absolute currents at a given absolute value of positive bias relative to the corresponding current at the negative bias, or *vice versa*.

Both anionic diodes and cationic diodes are useful, for example in combination to complement anion removal and cation removal. It is therefore of interest to explore surface modification of robust diode materials to control anion/cation semi-permeability. Following previous work on ionic diodes based on oxidized carbon nanofibers (CNFs, giving a cationic current rectifier), in this study the surface modification of CNF materials is attempted to provide an anionic current rectifier. Herein, a modified literature approach based on a hydrothermal reaction [25] is selected to produce a CNF material to provide a complementary material to the negatively charged CNF materials. Upon surface modification of CNFs with urea, generation (G3) poly (propylene imine) dendrimer and boric acid, a positively charged CNF material is obtained (forming stable and reproducible dispersions) and this is deposited as a "mat" onto a microhole in a PET substrate. When applying a positive bias voltage, behaviour a low current (due to electrolyte depletion and a "closed" diode) is observed. When the reverse negative voltage bias is applied, a high current is observed consistent with anion transport (due to electrolyte accumulation and an "open" diode). This anionic diode behaviour is mostly due to persistent protonation of dopant atoms in the modified CNF material, rendering the nanofiber walls positively charged. Such manipulation of perm-selectivity in carbon nanofiber mats can be useful in many applications including electrochemical water purification, ion selective membranes (e.g. for electrodialysis), or in ion removal/sensing.

2. Experimental Section

2.1. Reagents & Materials

The electrolyte salts used (including NaCl and NaOH) were obtained commercially in high purity ($\geq$ 98% purity), mineral acids (HCl, HNO_3, H_2SO_4) were of analytical grade, including urea, boric

acid and the carbon nanofibers employed (graphitized and iron-free, produced by floating catalyst vapour-growth method) were all purchased from Sigma Aldrich, South Africa. Agarose powder was purchased from ChemLab supplies, South Africa, and used without any further purification. Generation (G3) poly (propylene imine) (G3-PPI) dendrimer was purchased from SyMO-Chem, Eindhoven, Netherlands. The solvents including dried N,N-dimethylformamide (DMF) and ethanol used were of high purity (≥ 99.8%) bought from Sisco Research Laboratories Pvt. Ltd. (India). Poly (ethylene terephthalate) (PET) films of 6 μm thickness with laser-drilled microholes (of 5, 10, and 20 μm diameter) were obtained from Laser-Micro-Machining Ltd. (Birmingham, St. Asaph, United Kingdom) and used as substrates for ionic diode fabrication. All solutions were prepared using ultrapure water (18.2 MOhm cm at 22 °C).

2.2. Instrumentation

Transmission Electron Microscopy (TEM). High Resolution Transmission Electron Microscopy (HR-TEM) was performed using a JEOL JEM-2100F electron microscope (USA) with an accelerating voltage of 200 kV. Prior to the analysis, the carbon nanofibers were dispersed by briefly sonicating a small amount in ethanol using an ultrasonic bath (at room temperature). This technique was used to measure the diameter/size of the carbon nanofibers.

Scanning Electron Microscopy (SEM). The surface morphology of the carbon nanofiber films as well as cross-sectional images were examined using a Tescan Vega 3 XMU instrument (Czech Republic) scanning electron microscope with an acceleration voltage of 10 kV. A carbon nanofiber film/mat was made by drop-casting 10 μL dispersion of modified CNF in DMF (10% w/v) on top of PET substrate, after complete drying the film was carefully lifted off and broken in half, and one half placed vertically on a 12.7 mm diameter 45/90º chamfer specimen stub, previously coated with adhesive carbon tape.

Zeta potential measurements. The surface charge of the modified carbon nanofiber films was studied using a Malvern Zetasizer (South Africa), for this study 0.1 mg/ml dispersions were made

by dispersing 1 mg of CNFs or modified CNFs in respective solutions with different pH values (pH = 2, 4, 6, 8, 10, and 12) using sonication (1 h).

Electrochemical Measurements. All experiments were conducted using a conventional four-electrode configuration in a U-shaped cell (see Figure 1E). Electrochemical measurements were recorded using an Ivium CompactStat potentiostat (The Netherlands), equipped with 2 BASi Ag/AgCl (3 M KCl) electrodes serving as reference and sense electrodes, and 2 platinum wires (100 μm diameter) serving as counter and working electrodes, respectively. The current versus voltage (I−V) characteristics were measured (under conditions close to steady state) by sweeping the bias voltage from -2 to 2 V, at room temperature.

2.3. Procedure I.: Functionalisation of Carbon Nanofibers

The surface charge of carbon nanofibers can be modified using a literature recipe [25] to tune ionic conductivity. To achieve modification; about 250 mg of CNF powder was added to a 100 mL solution of generation-3 poly (propylene imine) dendrimer (G3-PPI, molecular weight 1686.8, SyMO-Chem) in water (5% w/v), and sonicated for 30 min to obtain a homogeneous dispersion. To the dispersed CNF/PPI solution, 500 mg urea and 500 mg boric acid were added, and the suspension was sonicated for another 30 min. About 80 mL of the homogeneous dispersion was transferred to a 100 mL Teflon-lined autoclave for hydrothermal reaction and heated at 180 ºC for 6 h. After cooling, the black suspension was filtered off through a 0.45 μm PVDF membrane and washed several times with ethanol and deionised water. The final product (modified CNFs) was obtained by drying at 60 ºC using a vacuum oven. Further experiments producing modified CNFs without hydrothermal treatment or without urea/boric acid were not successful in providing reproducible materials. Therefore the method based on urea/boric acid was chosen.

2.4. Procedure II.: Ionic Diode Fabrication

To a microhole on a 6 μm thick PET substrate (placed on glass slide previously coated with 1% w/v agarose gel) about 10 μL of a 10% w/v solution containing CNFs or modified CNFs in DMF (previously sonicated for 20 min) was drop-dried onto a single side of the PET film (over an area

of 1 cm^2 exactly where a single 5, 10, or 20 μm diameter microhole is situated). After slow drying and evaporation for 6 h at room temperature, reproducibly stable films of carbon nanomat on PET substrates form as a result of physical adhesion. Following this step, the films were rinsed with deionised water three times, and placed in a U-cell (Figure 1A), separating two symmetric electrolyte solutions (unless otherwise stated), with working (WE) and sense (SE) electrodes immersed on the side with carbon nanofiber film, and a reference (RE) and counter electrode (CE) immersed on the back side of the PET with no carbon nanofibers. When not in use, the ionic diode was stored soaked in deionized water.

3. Results and Discussion

3.1. Carbon Nanofiber Surface Characteristics

Film thickness and nanofiber packing. In order to determine the thickness of carbon nanofiber deposits/films, a cross-section image of the films was acquired using scanning electron microscopy (SEM). Figure 1A shows a side view image and the thickness of the film. The thickness of the CNF film was measured to be ~73 μm. Also seen from this image is that the carbon nanofibers forming the film, appear to be irregularly arranged or entangled (with porosity, voids, or channels between nanofibers). The film was deposited uniformly during deposition (with a glass rod used to uniformly distribute the nanofibers) onto a 6 μm thick PET substrate. Together with the CNF film the total membrane thickness is ~80 μm.

Nanofiber diameter and shape. In this study commercial carbon nanofibers (synthesised using vapor growing methods) were purchased from Sigma Aldrich. Before functionalisation, the nanofibers consisted of pure graphitic conical platelets (iron free), with an average nanofiber diameter around 100 nm, and lengths around 20 to 200 μm. Upon modification with G3-PPI, not much change occurred in terms of the diameter of the nanofibers (see Figure 1B). The diameter was measured to be around 118 nm, with the diameter of the hollow core ~60 nm, with walls around ~30 nm each. No new characteristics or changes in shape were observed for the surface functionalised nanofibers after functionalisation with G3-PPI dendrimer (in the presence of urea and boric acid). The nanofibers remained hollow, long and continuous.

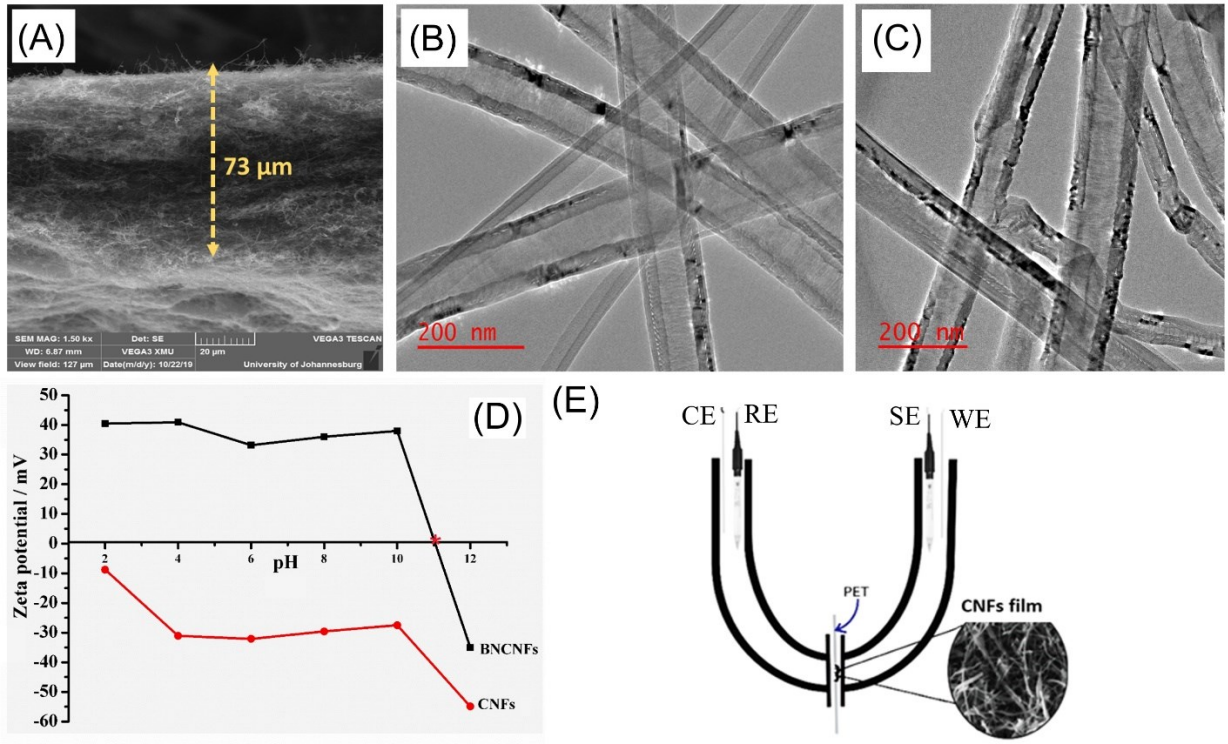

Figure 1. (A) Scanning electron microscopy images showing the cross-section or thickness for a boron and nitrogen doped carbon fiber film deposit. (B,C) Transmission electron micrograph for surface modified carbon nanofibers. (D) Zeta potential results. (E) Electrochemical setup with an asymmetric deposit of CNFs on a 10 µm pore on PET.

Surface charge properties. The surface characteristics of the carbon nanofibers before/after functionalisation were studied using a Malvern Zetasizer. The doped carbon nanofibers exhibit positive zeta potentials (implying stability and good dispersibility) in a pH range from 11 to 2 (Figure 1D). The point of zero charge was estimated at pH = 11.1. This contrasts to the pristine CNFs with predominantly negative surface charge and a point of zero charge close to pH 2.

3.2. Electrochemical Characterisation of Carbon Nanofiber Based Ionic Diodes

In order to test the efficiency, performance and reuse of the surface modified carbon nanofiber deposits on microholes of poly (ethylene terephthalate) immersed between two electrolyte

solutions, cyclic voltammetry and chronoamperometry were used. The I-V results reported are averages of three cycles, although only insignificant change was observed between the first scan and the third. Furthermore, reproducibility studies were carried by testing three different diodes of varying sizes (5 μm, 10 μm, and 20 μm) repeatedly at least three times. The 5 μm and 10 μm devices showed insignificant deviations in performance. For the 20 μm diameter device, up to ~20% variation in rectification performance occurred probably due to higher mechanical fragility. Persistent cationic diode behaviour was always observed for the pristine CNFs and anionic diode behaviour was always obtained for the modified CNFs.

Effect of electrolytes. Figures 2A shows I-V curves for carbon nanofibers deposited asymmetrically on a 20 μm sized cylindrical microhole in poly (ethylene terephthalate), immersed (from left and right) in three different types of electrolytes. The carbon nanofiber films always face the working electrode (see Figure 1E). For the pristine CNFs, a high current consistent with electrolyte accumulation ("open diode") is observed for positive voltage bias. This is consistent with cationic diode behaviour, and associated with negative surface charges. Similar behaviour is observed for HCl, NaCl, and NaOH, although the rectification ratio is clearly the highest for 10 mM NaOH. The increasing rectification ratio with increasing alkalinity (Figure 2C) may suggest possible functionalisation/oxidation of the surface due to deprotonation rendering the surface more negative.

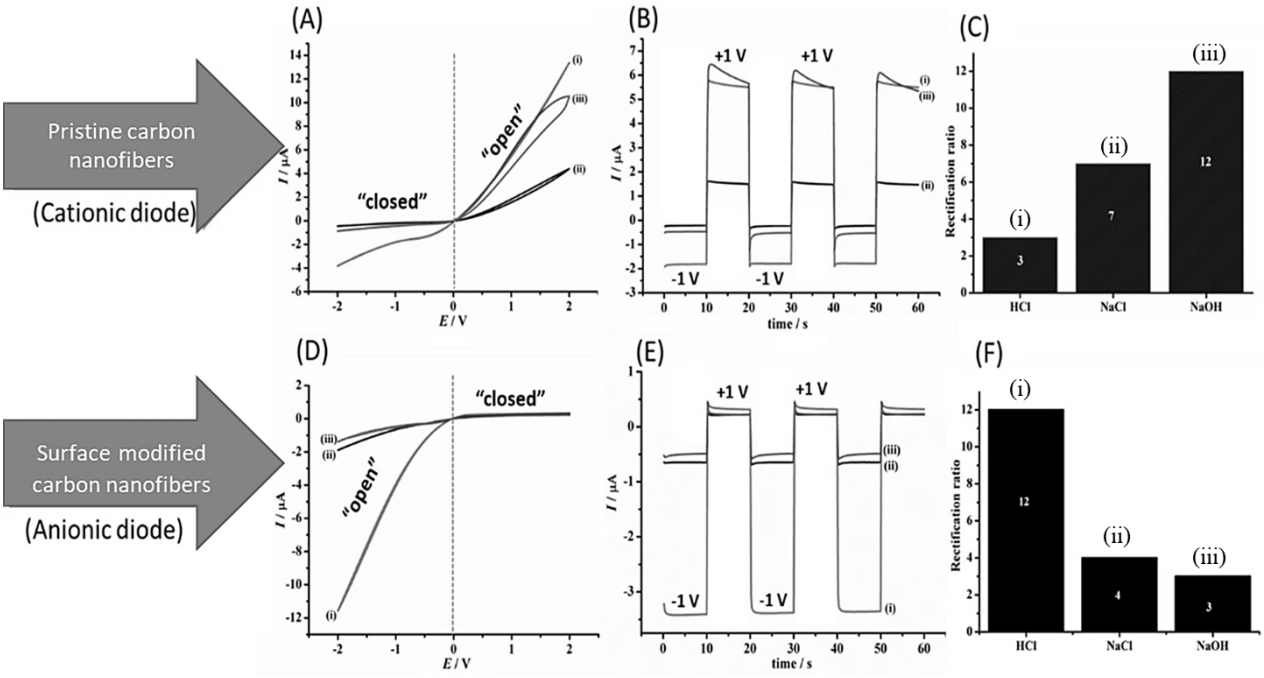

Figure 2. (A-C) Data (cyclic voltammetry and chronoamperometry) for asymmetrically deposited pristine carbon nanofiber deposits. (A) Cyclic voltammograms (scan rate 50 mV s^{-1}), (B) chronoamperometry data (stepping from + 1 to − 1 V), immersed in 10 mM aqueous (i) HCl, (ii) NaCl, (iii) NaOH. (C) Bar plot of rectification ratio data. (D-F) As above but for surface modified carbon nanofibers.

In chronoamperometry experiments, the on and off diode states (diode opening and closing) were achieved by applying +1/-1 V three times, in 10 second intervals. For the pristine carbon nanofibers, a high current (open diode) is always obtained when +1 V is applied, and low current (closed diode) is achieved when -1 V is applied. Upon surface-modification of the carbon nanofibers, the opposite pattern of behaviour is observed. A negative voltage bias such as -1 V gives rise to "open diode" and applying +1 V closes the diode. This is consistent with anionic diode behaviour, as a result of the positively charged carbon nanofiber surfaces. Switching diode behaviour can be achieved by application of voltages of different polarity [26]. The rectification ratio (Figure 2F) for currents obtained with ±1 V bias decreases in the order HCl > NaCl > NaOH, probably due to the higher positive surface charge in acidic media. This change in diode behaviour can be seen also in I-V curves (Figure 2D).

Schematic drawings (see Figure 3) are presented to further illustrate the cases of a cationic diode (for pristine carbon nanofibers, CNFs) and an anionic diode (for modified CNFs). For CNFs cationic diode behaviour is achieved in acid, neutral and basic media. The open state of a cationic diode is observed in the positive potential bias, associated with cations passing through the semi-permeable film and electrolyte accumulation in the microhole region. The closed state under these conditions results from electrolyte depletion in the microhole region. For the modified CNFs anionic diode behaviour is linked to fast anion transport through the film under negative applied bias. This results in electrolyte accumulation in the microhole region and an open state in the negative potential range.

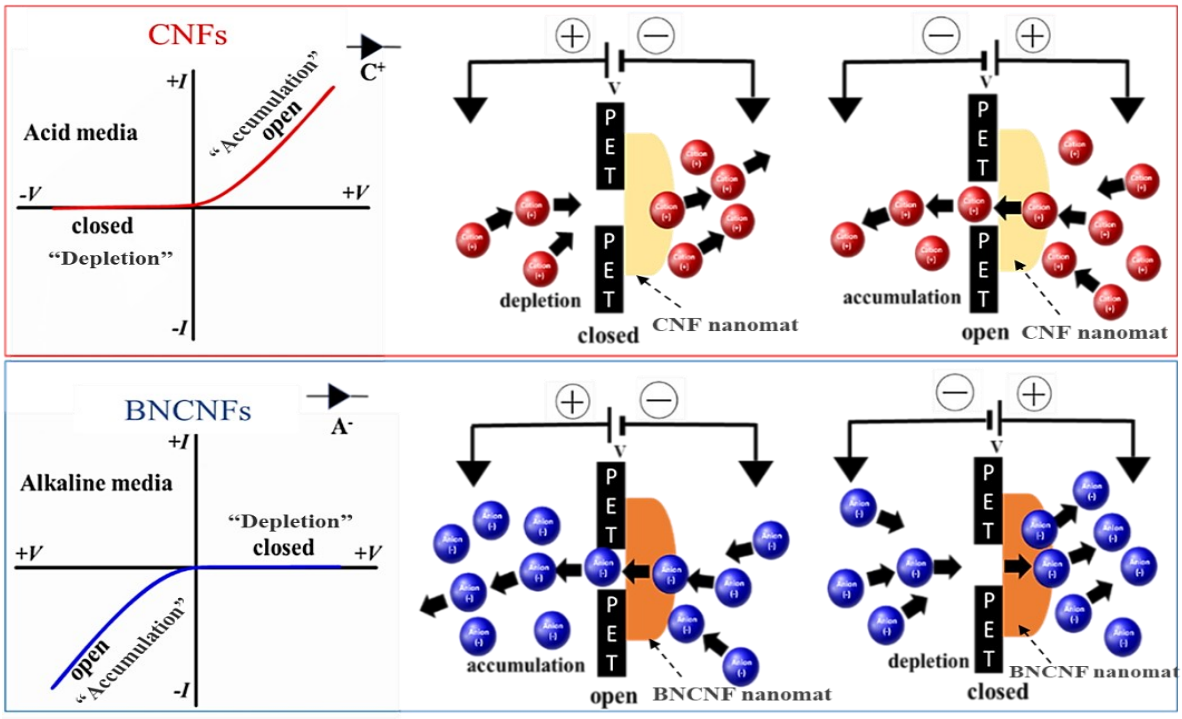

Figure 3. Schematic drawings for the four mechanistic cases of a cationic diode and an anionic diode under positive potential and negative potential polarisation, for pristine carbon nanofibers and surface modified carbon nanofibers.

Effects of microhole diameter. When the modified CNF ionic diode on microholes with diameter 5, 10, or 20 μm is immersed in 10 mM HCl solution, it is observed that the "open diode" current increases linearly with microhole area (see slope ≈ 2 in ln-ln plot in the inset in Figure 4A).

Chronoamperometry data suggest rapid switching between open and closed states for all three cases, but also a substantial effect of the microhole diameter on the rectification ratio. The rectification ratio increases when going from 5 μm to 10 μm to 20 μm diameter (Figure 4C). The reason for this behaviour is currently not clear but could be linked to the diffusion field changing from inside of the modified CNF film (for a small diameter) to outside the modified CNF film (for a bigger diameter). Furthermore, as the microhole size increases, so does the active surface covered by the modified carbon nanomat. If electrokinetic fluid flow affects the process in addition to ion flow, this could become more significant at increased diameter. The effects of electrokinetic flow have not been dissected and could affect currents.

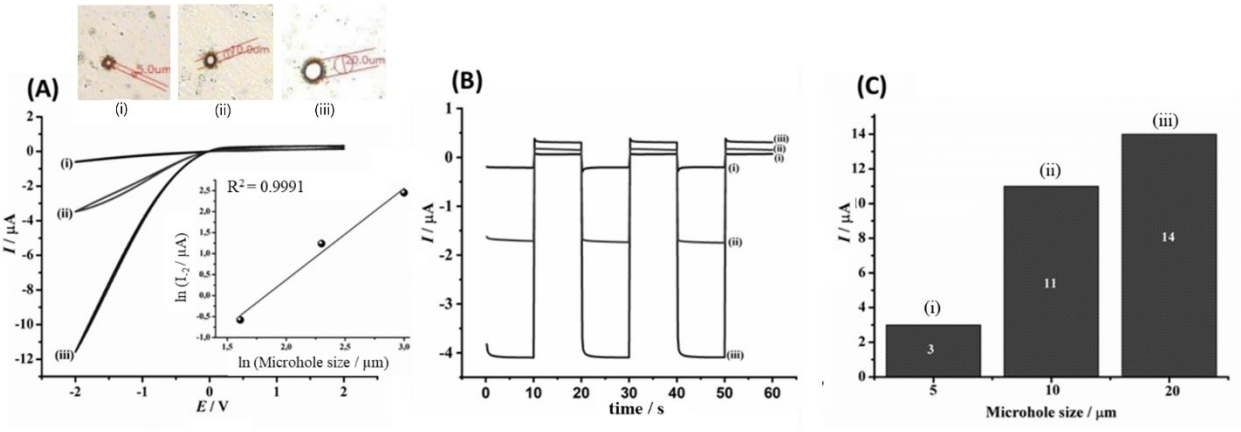

Figure 4. (A) Cyclic voltammograms (scan rate 50 mV s^{-1}) for modified CNFs deposited on a (i) 5, (ii) 10, and (iii) 20 μm diameter microhole in a PET substrate (see optical images inset) immersed in 10 mM aqueous HCl. Inset: plot of current vs microhole size. (B) Chronoamperometry data stepping from +1 to −1 V. (C) The rectification ratio (the absolute of the ratio of currents at +1 and −1 V) vs microhole diameter.

Effects of electrolyte ionic strength. Although the effects of scan rate during voltammetry experiments in aqueous HCl remains insignificant up to 1 Vs^{-1} (data not shown), the effect of the HCl concentration on the ionic diode response is significant (see Figure 5). When changing the HCl concentrations from 1 mM to 100 mM (equal electrolyte concentration left and right) both the open and the close state currents increase. At the same time, a loss of rectification ratio with ionic strength is observed (Figure 5C), presumably due to loss of semi-permeability at higher ionic

strength, an observation consistent with literature reports [27,28]. Empirically, the increase in open state current (at -2 V) is seen to have an approximately linear relationship with the square root of electrolyte concentration (see inset in Figure 5A). This can be explained at least tentatively by two counter acting effects: (i) a higher concentration will increase the current (as diffusional flux to the microhole) in a linear manner and (ii) the accumulation effect of electrolyte into the microhole region may be lower with higher external electrolyte concentration, thereby lowering the rectification effect. A further effect can be attributed to higher potential losses in the ionomer material with higher current [29]. Also, important to note is how little ionic diode switching time (ca. 1 s) is affected by the increase in electrolyte ionic strength.

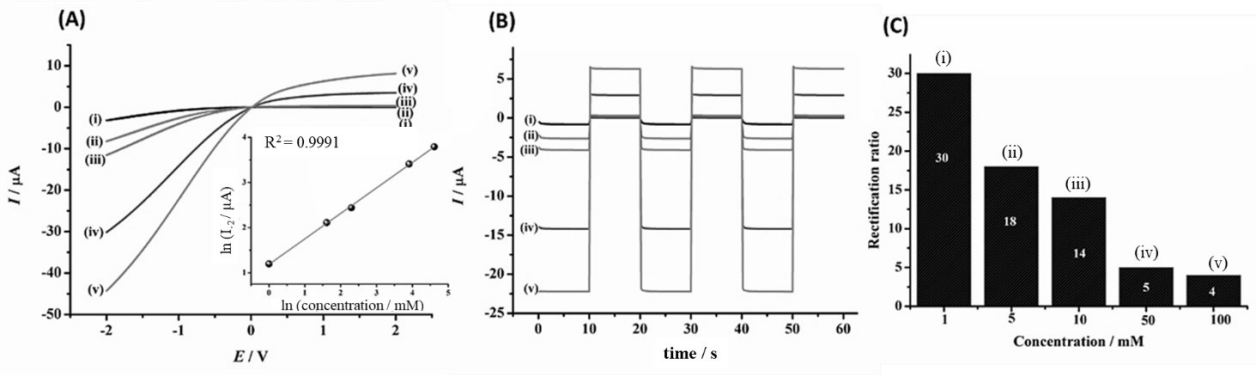

Figure 5. (A) Cyclic voltammograms (scan rate of 50 mV s^{-1}) for modified CNFs deposited on a 20 µm diameter microhole in a PET substrate immersed HCl concentration of (i) 1, (ii) 5, (iii) 10, (iv) 50, and (v) 100 mM. (B) Chronoamperometry data stepping from +1 to −1 V. (C) Plot of the rectification ratio (the absolute of the current at +1 V divided by the current at −1 V) vs concentration.

Electrochemical Impedance Spectroscopy. To further investigate switching of these ionic diodes, impedance spectroscopy measurements are carried out in a frequency range from 60 kHz to 0.1 Hz. The four-electrode two-compartment cell (Figure 1E) is employed and all data could be analysed based on a circuit model shown in Figure 6A. From data Figure 6A, it can be observed that applying different DC bias to the diode results in differently shaped Nyquist plots with two main features: a high frequency intercept is associated with residual electrolyte resistance (R_S) and a high frequency semi-circle is linked to the high frequency resistance of the diode material (R_1)

in parallel to the PET film capacitance (C_1). Charging of C_1 is counter-acted by discharge through R_1. A second slower process is associated with a flow of ions through the diode (R_2) and an apparent capacitance (C_2) that includes effects such as external concentration polarisation (accumulation and depletion of electrolyte in the microhole). R_2 also has be regarded as an average due to a constantly changing (potential dependent) ion flow resistance and rectification at lower frequencies. However, a full model for this ionic diode switching process still needs to be developed. Here, data are interpreted as time constants at phenomenological level.

In the presence of 10 mM HCl, applying a positive DC bias of +0.1 V for the modified CNF material on a 20 µm microhole results in two semicircles distinct for PET film charging and for diode switching (see Table 1). The apparent first time constant $\tau_1 = R_1 \times C_1$ is approximately 0.15 ms independent of the applied bias voltage consistent with charging of the PET film. The apparent second time constant $\tau_2 = R_2 \times C_2$ changes from approximately 5 ms (+0.1 V) to 0.2 ms (-0.1 V) consistent with a slightly faster switching for the “open” diode.

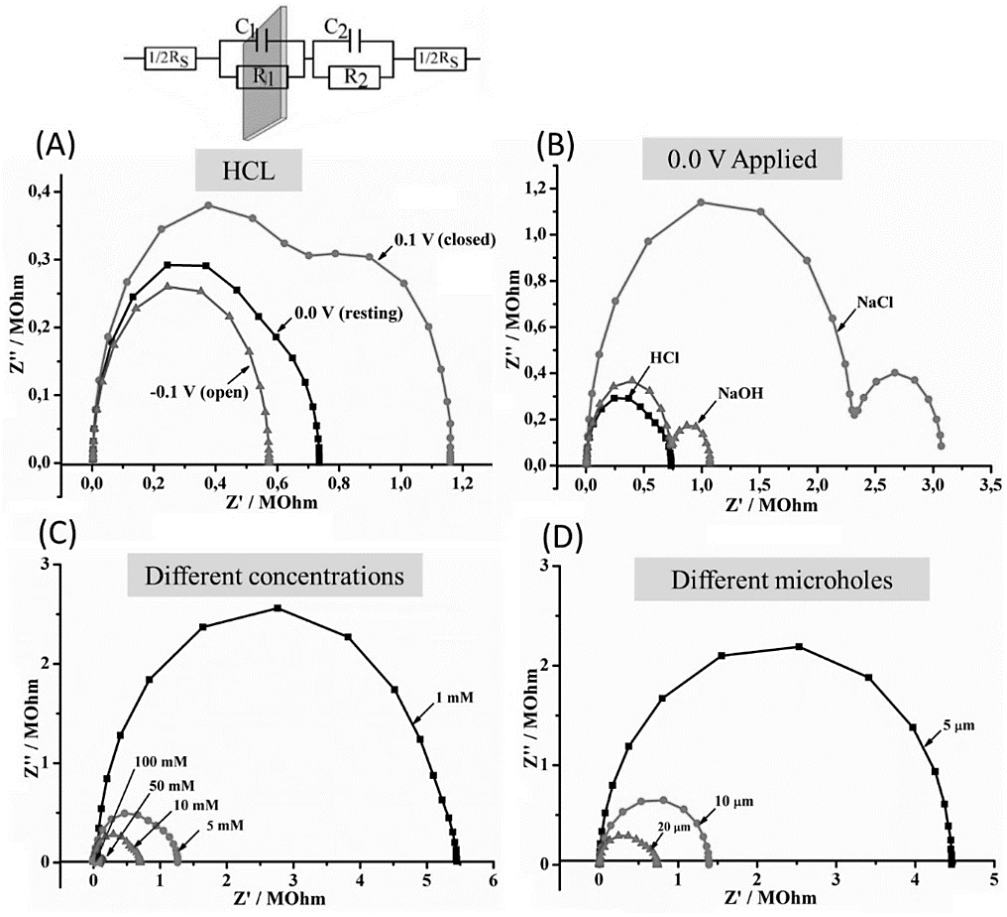

Figure 6. (A) Nyquist plots showing the effect of applied voltage for a modified CNF diode (on a 20 µm microhole in a PET substrate) immersed in 10 mM aqueous HCl (in the frequency regime 60 KHz – 0.1 KHz, 100 mV amplitude). (B) Nyquist plot showing the effect of electrolyte and acidity on resistivity of the modified CNF diode when 0 V is applied, the diode is the same as that described above. (C) Shows the effect of increasing HCl concentration on diode resistivity, while (D) shows Nyquist plots depicting the effect of microhole size on resistivity, an R(RC)(RC) circuit is used to fit and model all data.

When comparing the behaviour for different electrolytes at 0 V bias (10 mM HCl, 10 mM NaCl, and 10 mM NaOH, see Figure 6B), the time constants τ_1 remain approximately 0.2 ms, whereas τ_2 changes from 6 ms (HCl) to 500 ms (NaCl) to 100 ms (NaOH). When developing the electrolyte accumulation and depletion zone in the microhole region, both the mobility of the anion (passing through the semi-permeable material) and the mobility of the cation (diffusion from the electrolyte phase) are implicated. This explains the trends in apparent time constant associated with relatively fast diffusion due to protons and to lesser extent due to hydroxide.

Table 1. EIS data for a modified CNF diode coated on a 20 μm diameter microhole at 0 V applied bias, as well as data when the diode is "open" (+0.1 V bias) and "closed" (-0.1 V bias). The frequency range is from 60 kHz to 100 Hz, amplitude 100 mV. Both the high and low frequency semi-circular features of the Nyquist plot data are analysed (fitting errors in brackets).

Conditions	**R_S / KOhm**	**R_1 / MOhm**	**R_2 / MOhm**	**C_1 / nF**	**C_2 / nF**
Modified CNF diode (different applied voltages)					
0 V	3.07 (4.2%)	0.19 (9.5%)	0.54 (3.3%)	0.54 (1.3%)	11.7 (23%)
+0.1 V	3.10 (6.7%)	0.49 (5.7%)	0.67 (3.8%)	0.56 (1.6%)	8.94 (15%)
-0.1 V	3.05 (2.9%)	0.20 (28%)	0.37 (20.3%)	0.63 (12.7%)	0.28 (27%)
Different electrolytes (0 V Applied)					
10 mM HCl	3.07 (4.2%)	0.19 (9.5%)	0.54 (3.3%)	0.54 (1.3%)	11.7 (23%)
10 mM NaCl	9.06 (2.8%)	0.77 (7.6%)	2.30 (1.3%)	0.52 (1.1%)	224 (15%)
10 mM NaOH	4.41 (5.4%)	0.34 (6.2%)	0.73 (1.6%)	0.52 (1.5%)	146 (14%)

Table 2. Summary of EIS data for different concentrations of HCl for a modified CNF film on a 20 μm diameter microhole, when 0 V is applied, also included is data when microhole size is varied for a 10 mM HCl solution (frequency range 60 kHz – 100 Hz, amplitude 100 mV, both the high frequency and the low frequency semi-circular parts of the Nyquist plot data is analysed (fitting errors in brackets).

Conditions	**R_S / KOhm**	**R_1 / MOhm**	**R_2 / MOhm**	**C_1 / nF**	**C_2 / nF**
Modified CNF diode (0 V applied)					
1 mM HCl	50.88 (6.6%)	0.32 (14%)	5.08 (11%)	0.48 (4.6%)	9.17 (25%)
5 mM HCl	9.19 (1.8%)	0.37 (7.4%)	0.88 (3.2%)	0.46 (1.3%)	7.09 (17%)

10 mM HCl	5.95 (2.9%)	0.15 (7.6%)	0.54 (2.0%)	0.45 (0.9%)	1.91 (20%)
50 mM HCl	0.59 (8.5%)	0.017 (17%)	0.11 (2.8%)	0.45 (1.3%)	1.10 (13%)
100 mM HCl	0.211 (16%)	0.01 (19%)	0.059 (3.2%)	0.45 (1.7%)	0.82 (18%)
Different microholes					
5 µm	4.03 (1.8%)	4.40 (0.9%)	0.56 (16%)	0.52 (2.3%)	7.48 (28%)
10 µm	4.48 (1.1%)	0.10 (14%)	0.29 (22%)	0.58 (21%)	10.3 (25%)
20 µm	3.07 (4.2%)	0.19 (9.5%)	0.078 (3.3%)	0.54 (1.3%)	11.7 (23%)

When changing the HCl electrolyte concentration and at 0 V bias, Figure 6C, and table 2 show that τ_1 decreases (due to R_1 decreasing) with higher HCl concentration. For τ_2 the value systematically decreases; 45, 6.3, 0.95, 0.12, 0.05 ms for concentrations ranging from 1 mM to 100 mM HCl. Indicating clearly, that the accumulation and depletion of electrolyte in the microhole region is considerably faster in the presence of a higher concentration of electrolyte. When changing the microhole diameter, diode resistivity (R_2) decreases with increasing microhole size, while diode capacitance (C_2) increased with increasing microhole size. The τ_2 values slightly but systematically decrease in the order; 4.2, 3.0, 0.93, for the 5, 10, and 20 µm diodes, suggesting slightly faster accumulation and depletion of electrolyte in the microhole region, when larger microholes are used. This trend seems to be linked to resistance changes. When comparing to literature values for typical switching times for example for nanofluidic ionic diodes [30], values of typically 1 s are commonly observed.

4. Conclusion

Carbon nanofibers have been successfully surface modified with amine functional groups to form a positively charged carbon nanomat (modified CNFs) using a hydrothermal method. Pristine

carbon nanofibers are shown to be active as cationic rectifiers (negative surface charge), whilst surface modification changes the behaviour into anionic rectifier (positive surface charge). CNF mats of typically 73 µm thickness on a PET substrate with microhole are shown to provide stable rectifier effects in different types of electrolytes, at different pH values, as a function of ionic strength, and for different microhole diameters. A 20 µm diameter microhole device immersed in 10 mM HCl shows the strongest rectifier effects. However, the observed rectification ratio of typically 10 is not sufficient and further study will be necessary to improve rectification. Most likely, charge density and porosity in the carbon mat are both crucial. By compressing or cross-linking the carbon material, better rectification effects should be possible in the future. Another important factor is durabillity during operation and more work will be necessary to test and improve this.

From the impedance studies, it was shown that the calculated time constants (the measure of switching time of the diode) can be understood as strongly dependent on electrolyte strength and on the diameter of the microhole used. Impedance data reveals that faster diode switching for this type of ionic diode material is encountered at higher electrolyte strengths and upon using bigger microholes in diode fabrication. In future work, the effects of multi-valent cations or aniosn should be studied.

The methodology of surface-modification could in the future be further developed to give improved rectifier behaviour also for neutral solution and for the case of 0.5 M NaCl to allow application in desalination applications. Ideally, a combination of materials for simultaneous cationic diode and anionic diode combinations (based on two different types of surface modifications) will be desirable. Both the surface charge density and the density of packing of the CNF materials will have to be optimised.

Acknowledgements

L.T. thanks the Global Excellence and Stature, University of Johannesburg for Doctoral Scholarship. DST/Mintek Nanotechnology Innovation Centre, University of Johannesburg, South Africa; the Water Research Commission, (Grant number: K5/2567) South Africa; the National Research Foundation (CPRR Grant number: 118546), South Africa are acknowledged for their financial support.

References

[1] Z. Zhang, L. Wen, and L. Jiang, Bioinspired smart asymmetric nanochannel membranes, *Chemical Society Reviews* 47 (2) (2018) 322-356.

[2] J. Experton, X. Wu, and C. R. Martin, From Ion Current to Electroosmotic Flow Rectification in Asymmetric Nanopore Membranes, *Nanomaterials (Basel, Switzerland)* 7 (12) (2017) 445.

[3] W. J. Lan *et al.*, Voltage-Rectified Current and Fluid Flow in Conical Nanopores, *Accounts of Chemical Research* 49 (11) (2016) 2605-2613.

[4] W. Guo, Y. Tian, and L. Jiang, Asymmetric Ion Transport through Ion-Channel-Mimetic Solid-State Nanopores, *Accounts of Chemical Research* 46 (12) (2013) 2834-2846.

[5] W. Guan, S. X. Li, and M. A. Reed, Voltage gated ion and molecule transport in engineered nanochannels: theory, fabrication and applications, *Nanotechnology* 25 (12) (2014) 122001.

[6] H. Chun and T. D. Chung, Iontronics, *Annual Review of Analytical Chemistry* 8 (1) (2015) 441-462.

[7] G. Pérez-Mitta, M.E. Toimil-Molares, C. Trautmann, W.A. Marmisollé, O. Azzaroni, Molecular Design of Solid-State Nanopores: Fundamental Concepts and Applications, *Advanced Materials* 31(37) (2019) 1901483.

[8] L. Tshwenya, F. Marken, and O. A. Arotiba, Carbon Nanofibers Provide a Cationic Rectifier Material: Specific Electrolyte Effects, Bipolar Reactivity, and Prospect for Desalination, *ChemElectroChem* 6 (12) (2019) 3145-3153.

[9] G. Pérez-Mitta, A.G. Albesa, C. Trautmann, M.E. Toimil-Molares, O. Azzaroni, Bioinspired integrated nanosystems based on solid-state nanopores: "Iontronic" transduction of biological, chemical and physical stimuli, *Chemical Science* 8 (2) (2017) 890-913.

[10] J. Gao, W. Guo, D. Feng, H. Wang, D. Zhao, and L. Jiang, High-Performance Ionic Diode Membrane for Salinity Gradient Power Generation, *Journal of the American Chemical Society* 136 (35) (2014) 12265-12272.

[11] Q. Wang, H. Wang, X. Fan, and J. Zhai, Biological recognition with bio-inspired smart nanopores and nanochannels based on polymer membrane, *Science of Advanced Materials* 7 (10) (2015) 2147-2167.

[12] B. Lovrecek, A. Despic, and J. Bockris, Electrolytic junctions with rectifying properties, *The Journal of Physical Chemistry* 63 (5) 750-751.

[13] E. Madrid *et al.*, Metastable Ionic Diodes Derived from an Amine-Based Polymer of Intrinsic Microporosity, *Angewandte Chemie International Edition* 53 (40) (2014) 10751-10754.

[14] D. He *et al.*, A cationic diode based on asymmetric Nafion film deposits, *ACS Applied Materials & Interfaces* 9 (12) (2017) 11272-11278.

[15] S. Park and G. Yossifon, Electrothermal based active control of ion transport in a microfluidic device with an ion-permselective membrane, *Nanoscale* 10 (24) (2018) 11633-11641.

[16] Y. Green, Y. Edri, and G. Yossifon, Asymmetry-induced electric current rectification in permselective systems, *Physical Review E* 92 (3) (2015) 033018.

[17] E. Madrid *et al.*, Water desalination concept using an ionic rectifier based on a polymer of intrinsic microporosity (PIM), *Journal of Materials Chemistry A* 3 (31) (2015) 15849-15853.

[18] B. R. Putra, M. Carta, R. Malpass-Evans, N. B. McKeown, and F. Marken, Potassium cation induced ionic diode blocking for a polymer of intrinsic microporosity | nafion “heterojunction” on a microhole substrate, *Electrochimica Acta* 258 (2017) 807-813.

[19] B. D. Aaronson, D. Wigmore, M. A. Johns, J. L. Scott, I. Polikarpov, and F. Marken, Cellulose ionics: switching ionic diode responses by surface charge in reconstituted cellulose films, *Analyst* 142 (19) (2017) 3707-3714.

[20] B. R. Putra, K. J. Aoki, J. Chen, and F. Marken, Cationic Rectifier Based on a Graphene Oxide-Covered Microhole: Theory and Experiment, *Langmuir* 35 (6) (2019) 2055-2065.

[21] B. R. Putra *et al.*, Processes associated with ionic current rectification at a 2D-titanate nanosheet deposit on a microhole poly (ethylene terephthalate) substrate, *Journal of Solid State Electrochemistry* 23 (4) (2019) 1237-1248.

[22] L. Tshwenya, F. Marken, K. Mathwig, and O. A. Arotiba, Switching Anionic and Cationic Semi-Permeability in Partially Hydrolyzed Polyacrylonitrile: A pH-Tunable Ionic Rectifier, *ACS Applied Materials & Interfaces* 12 (2) (2020) 3214-3224.

[23] K. Mathwig, B. D. Aaronson, and F. Marken, Ionic transport in microhole fluidic diodes based on asymmetric ionomer film deposits, *ChemElectroChem* 5 (6) (2018) 897-901.

[24] L. Ye and Z. Feng, 14 - Polymer electrolytes as solid solvents and their applications, *Polymer Electrolytes*, Woodhead Publishing (2010) 550-582.

[25] L. Chen *et al.*, Hydrothermal preparation of nitrogen, boron co-doped curved graphene nanoribbons with high dopant amounts for high-performance lithium sulfur battery cathodes, *Journal of Materials Chemistry A* 5 (16) (2017) 7403-7415.

[26] G. Pérez-Mitta *et al.* An All-Plastic Field-Effect Nanofluidic Diode Gated by a Conducting Polymer Layer. *Advanced Materials* 29 (28) (2017) 1700972.

[27] L. Tshwenya *et al.*, Cationic diodes by hot-pressing of Fumasep FKS-30 ionomer film onto a microhole in polyethylene terephthalate (PET), *Journal of Electroanalytical Chemistry* 815 (2018) 114-122.

[28] G. Laucirica *et al*., Shape matters: Enhanced osmotic energy harvesting in bullet-shaped nanochannels, *Nano Energy* 71 (2020) 104612.

[29] B.R. Putra, K.J. Aoki, J.Y. Chen, F. Marken, Cationic rectifier based on a graphene oxide-covered microhole: theory and experiment, *Langmuir* 35 (2019) 2055-2065.

[30] G. Laucirica, V.M. Cayon, Y.T. Terrones, M.L. Cortez, M.E. Toimil-Molares, C. Trautmann, W.A. Marmisolle, O. Azzaroni, Electrochemically addressable nanofluidic devices based on PET nanochannels modified with electropolymerized poly-o-aminophenol films, Nanoscale 12 (2020) 6002-6011.